OPTIMIZING HEAT TRANSFER IN LAMINAR CHANNEL FLOW USING INCLINED INVERTED *L*-SHAPED OBSTACLES

by

Omolayo M. IKUMAPAYI[a], Noureddine KAID[b], Samia LARGUECH[c], Younes MENNI[b,d], Mustafa BAYRAM[e*], Abiodun BAYODE[a], Tin Tin TING[f,g], Ali AKGUL[e,h,i,j,k], and Salih OZER[l]

[a] Department of Mechanical Engineering, Northwest University, Potchefstroom, South Africa
[b] Department of Mechanical Engineering, Institute of Technology, University Center Salhi Ahmed Naama (Ctr. Univ. Naama), Naama, Algeria
[c] Department of Electrical Engineering, College of Engineering, Princess Nourah bint Abdulrahman University, Riyadh, Saudi Arabia
[d] College of Technical Engineering, National University of Science and Technology, Dhi Qar, Iraq
[e] Department of Computer Engineering, Biruni University, Istanbul, Turkey
[f] Faculty of Data Science and Information Technology, INTI International University, Nilai, Malaysia
[g] School of Information Technology, UNITAR International University, Selangor, Malaysia
[h] Department of Electronics and Communication Engineering, Saveetha School of Engineering, SIMATS, Chennai, Tamilnadu, India
[i] Siirt University, Art and Science Faculty, Department of Mathematics, Siirt, Turkey
[j] Department of Mathematics, Mathematics Research Center, Near East University, Nicosia/Mersin, Turkey
[k] Applied Science Research Center, Applied Science Private University, Amman, Jordan
[l] Mus Alparslan University, Mechanical Engineering, Mus, Turkiye

Original scientific paper
https://doi.org/10.2298/TSCI2504219I

This study numerically investigates the influence of obstacle inclination and flow rate on the convective heat transfer performance in a 3-D rectangular channel equipped with periodically arranged inverted L-shaped obstacles. Using the finite element method, simulations were conducted for laminar flow conditions across a range of Reynolds numbers (Re = 20-600) and obstacle inclination angles (30°, 45°, and 60°). Water was used as the working fluid, and thermal enhancement was evaluated using temperature contours, local Nusselt number distributions, and average Nusselt values. Results reveal that increasing both Reynolds number and obstacle inclination significantly enhances thermal performance. The 60° configuration consistently yielded the highest local and average Nusselt numbers, with up to 99.5% improvement over the 30° case at Re = 600. Temperature fields confirmed enhanced vortex formation, mixing, and wall impingement in steeper geometries. This study highlights the potential of obstacle inclination as a passive enhancement technique in compact thermal systems operating under laminar flow conditions.

Key words*: water flow, heat transfer, L-geometry, numerical study, CFD*

[*] Corresponding author, e-mail: mustafabayram@biruni.edu.tr

Introduction

Improving convective heat transfer in internal flows is essential for advancing thermal systems like compact heat exchangers and solar collectors. Among passive methods, inserting obstacles into the flow path stands out for its simplicity and effectiveness. By disrupting boundary-layers, generating vortices, and promoting fluid mixing, these obstacles, ranging from basic geometries to porous and magnetically influenced structures, significantly boost thermal performance without requiring additional energy input [1]. Numerous studies have examined this approach using both experimental and numerical methods. Moradi and D'Orazio [2] applied the lattice Boltzmann method (LBM) to analyze the role of obstacle size and arrangement in porous channels, while Mohankumar and Prakash [3] investigated elliptical obstacles in stepped geometries. The influence of fluid rheology was addressed by Nitin and Chhabra [4] for power-law fluids flowing past rectangular obstacles. In mini-channel and micro-channel configurations, Hameed *et al*. [5] evaluated the thermal and hydraulic performance of serpentine channels with embedded obstacles under laminar flow, while Akbari *et al*. [6] and Alshukri *et al*. [7] demonstrated the heat transfer enhancement effects of structured and staggered obstacles using nanofluids in turbulent and two-phase flow conditions. Ghoulam *et al*. [8] examined detached obstacles in ducts, and Akhter *et al*. [9] studied entropy generation in porous-wavy channels with triangular blocks under magnetic fields. Yaseen *et al.* [10] and Ren *et al*. [11] explored the sensitivity of obstacle location and thermal conductivity in enclosures and solar chimneys, respectively, while Khan *et al.* [12] analyzed MHD and Joule heating effects on cylindrical obstacles. Optimization and design of porous arrays were addressed by Mirahsani *et al*. [13], and mist cooling over obstacles was simulated by Pakhomov [14]. Further, Han *et al*. [15] examined unilateral obstruction length in micro-channels, and Barman and Dash [16] evaluated obstacle position in stepped turbulent channels. The MHD effects were studied by Tassone *et al*. [17], and rarefied gas dynamics were modeled by Hammid *et al*. [18] using LBM. Conjugate heat transfer involving wall-mounted obstacles was presented by Pirouz *et al*. [19], and conductive *L*-shaped obstacles under magnetic fields were examined by Selimefendigil and Oztop [20]. Applications in solar thermal systems have also benefited from obstacle-based enhancements. Salmi *et al*. [21], Maouedj *et al*. [22], and Menni *et al.* [23] investigated vortex generators and baffles in solar channels, while Chamkha *et al*. [24] and Medjahed *et al.* [25] focused on thermal performance improvements using *S*-shaped fins and staggered *T*-shaped baffles. Overall, these studies confirm that strategically placed obstacles, regardless of geometry, material, or scale, significantly enhance heat transfer in internal flow systems across a wide range of configurations and operating conditions.

Improving heat transfer in laminar channels is essential for efficient thermal system design. Inverted *L*-shaped obstacles are effective passive elements. However, the influence of their inclination angle on heat transfer and fluid-flow remains underexplored. This study examines how varying the inclination of these obstacles affects thermal and hydraulic performance, with the goal of identifying configurations that enhance heat transfer while limiting flow resistance.

Mathematical and numerical modelling

The computational domain consists of a 3-D rectangular channel with periodically arranged inverted *L*-shaped obstacles inclined at different angles (30°, 45°, and 60°), as illustrated in fig. 1. The obstacles are attached to both the upper and lower channel walls, and additional central obstacles are placed within the flow passage. The working fluid is water, modeled as an incompressible, Newtonian fluid with constant thermophysical properties. The flow is assumed

to be steady and laminar, with no body forces, radiation, or buoyancy effects considered. Heat transfer occurs through forced convection, and the channel walls are assumed to be solid and stationary.

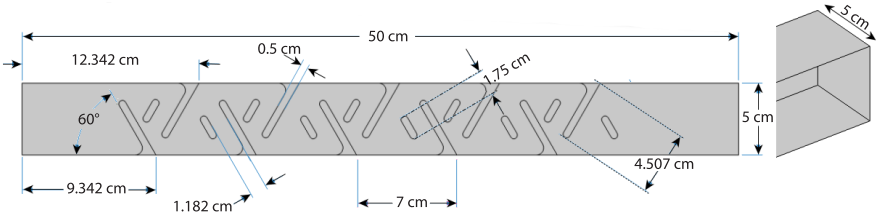

Figure 1. The 3-D channel with inclined inverted *L*-shaped obstacles on both walls

The conservation equations for mass, momentum, and energy govern the behavior of the fluid-flow and heat transfer in the domain. These equations, under the aforementioned assumptions, are given in Cartesian co-ordinates.

Continuity equation:

$$\nabla\vec{\mathrm{u}} = 0 \tag{1}$$

Momentum equation:

$$\rho\left(\vec{\mathrm{u}}\nabla\right)\vec{\mathrm{u}} = -\nabla p + \mu\nabla^2\vec{\mathrm{u}} \tag{2}$$

Energy equation:

$$\rho C_p\left(\vec{\mathrm{u}}\nabla\mathrm{T}\right) = k\nabla^2 T \tag{3}$$

where $\vec{\mathrm{u}} = (u, v, w)$ is the velocity vector in the x-, y-, and z-directions, p – the pressure, ρ – the fluid density, μ – the dynamic viscosity, C_p – the specific heat capacity, and k – the thermal conductivity of water. The boundary conditions applied to the computational domain are as follows and are illustrated in fig. 2. At the inlet, a uniform velocity profile is imposed along with a constant inlet temperature. The outlet is treated with a zero-gradient condition for all variables, and the pressure is set to atmospheric (gauge pressure = 0). The lower wall is subjected to no-slip and isothermal boundary conditions, representing a constant-temperature surface. In contrast, the upper wall is treated as no-slip and adiabatic, indicating that no heat exchange occurs across this surface.

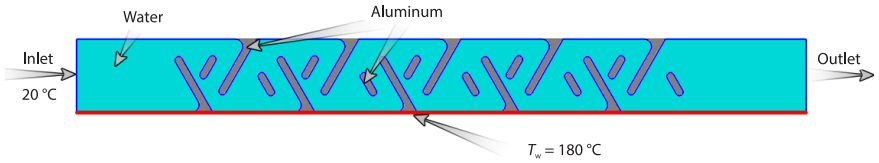

Figure 2. Boundary conditions applied to the 3-D computational domain

The computational mesh for the 3-D channel with inclined inverted *L*-shaped obstacles is a hybrid unstructured grid consisting of 1485285 elements, including 1291773 tetrahedral and 193512 prismatic cells. Surface discretization uses 107467 triangular and 276 quadrilateral elements. Prismatic layers near the walls enhance boundary-layer resolution. The mesh shows good overall quality (average 0.6795), though a minimum quality of 0.01356 suggests localized refinement issues. This fine mesh, illustrated in fig. 3, ensures accurate capture of flow and thermal gradients around the complex geometry.

The governing equations are solved using the finite element method. Convergence criteria are set to 10^{-6} for the continuity and momentum equations, and 10^{-8} for the energy

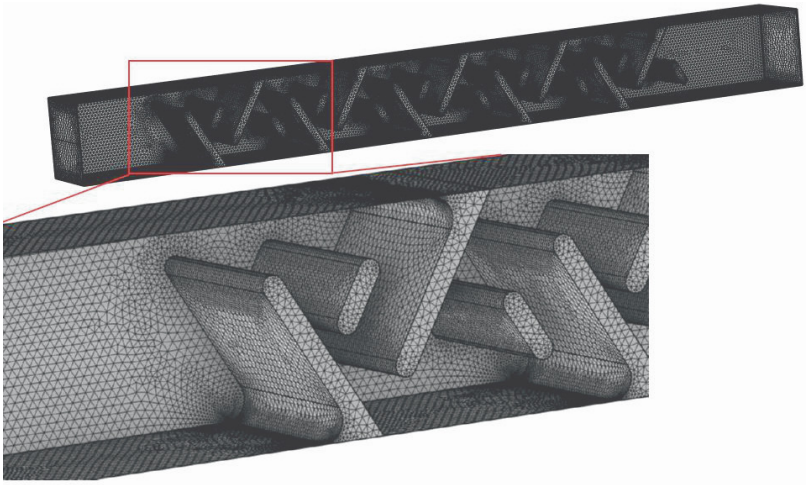

Figure 3. Hybrid unstructured mesh for the domain with inclined inverted *L*-shaped obstacles

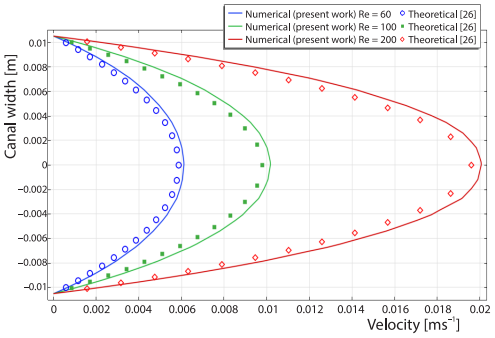

Figure 4. Velocity profile validation at Reynolds numbers 60, 100, and 200

equation ensure accurate resolution of thermal gradients. The solution is considered converged when all residuals fall below these specified thresholds and the monitored average Nusselt number reaches a stable value, indicating numerical consistency and solution reliability. To validate the accuracy of the numerical model, a reference case of laminar flow in a smooth, unobstructed channel was simulated. The computed velocity profiles showed excellent agreement with the exact parabolic solution described by Comolet [26], as illustrated in fig. 4 for Reynolds numbers of 60, 100, and 200. This confirms the model's ability to capture fundamental laminar flow behavior and establishes confidence in its application more complex configurations.

Results and discussion

Figure 5 provides a visual representation of temperature fields within the 3-D channel for three obstacle inclination angles (30°, 45°, and 60°) at Reynolds numbers of 20, 100, and 600. The temperature contours clearly reveal how obstacle inclination and flow rate interact to shape the thermal behavior and influence heat transfer effectiveness along the heated lower wall.

At Re = 20, where the flow is in the laminar regime, all three inclination cases exhibit broad thermal boundary-layers and smooth temperature gradients. Among them, the configuration with a 30° inclination shows more effective distribution of cooler fluid toward the heated lower wall. As illustrated in fig. 5(a), this is reflected in more uniform temperature contours near the wall and reduced thermal stagnation behind the obstacles. The gentler inclination allows the fluid to pass with minimal separation while still disturbing the boundary-layer enough to promote moderate heat transfer, offering an optimal balance for low flow scenarios.

As the flow rate increases to Re = 100, the role of convective transport becomes more dominant, and the influence of obstacle inclination becomes more evident. As shown in fig. 5(b), the 45° inclined obstacles exhibit enhanced heat removal, marked by stronger fluid mixing and sharper thermal gradients along the heated lower wall. Vortex formation around the inclined edges significantly boosts local convection, particularly just downstream of the obstacles. In contrast, the 30° inclination begins to exhibit thermal accumulation due to insufficient flow disturbance, while the 60° case generates larger re-circulation zones that reduce effective thermal contact and limit downstream cooling efficiency.

At the highest flow rate of Re = 600, convective heat transfer becomes dominant, resulting in thin thermal boundary-layers and sharply defined temperature contours. As illustrated in fig. 5(c), the 60° inclination proves most effective in this regime. The steeper angle introduces greater flow disruption, generating vigorous vortex activity and strong wall impingement that markedly reduce surface temperatures and enhance overall heat removal. The temperature fields reveal deeper penetration of cooler fluid along the channel length with minimal thermal layering compared to the lower inclination cases. This indicates intensified fluid-wall interaction and more efficient utilization of the heated surface for convective heat dissipation.

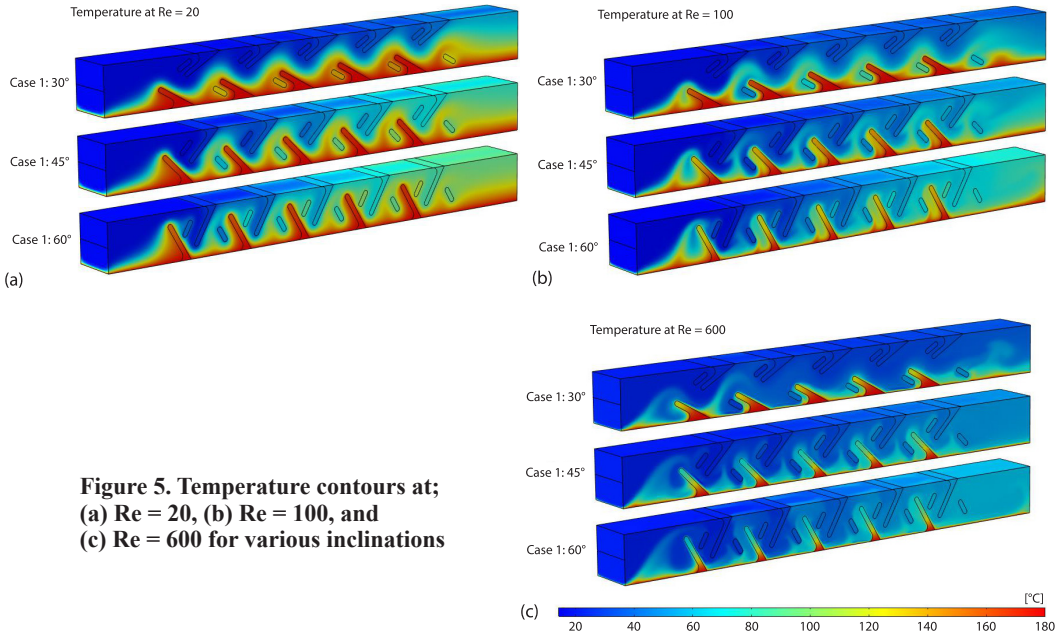

Figure 5. Temperature contours at; (a) Re = 20, (b) Re = 100, and (c) Re = 600 for various inclinations

The distribution of the local Nusselt number provides insight into the spatial heat transfer behavior along the heated wall, reflecting how the flow interacts with the periodically arranged inverted *L*-shaped obstacles. As illustrated in fig. 6, across all Reynolds numbers (Re = 20, 100, and 600), the local Nusselt number exhibits a clear periodic pattern. Each peak corresponds to the presence of an obstacle, where flow separation, vortex formation, and wall impingement enhance local heat transfer. A prominent inlet effect is observed in all cases, characterized by a high Nusselt number at the channel entrance due to undeveloped thermal boundary-layers, followed by a sharp drop as the boundary-layer thickens.

At Re = 20, the flow remains laminar, with heat transfer dominated by conduction rather than convection. As shown in fig. 6(a), the local Nusselt number varies smoothly, with

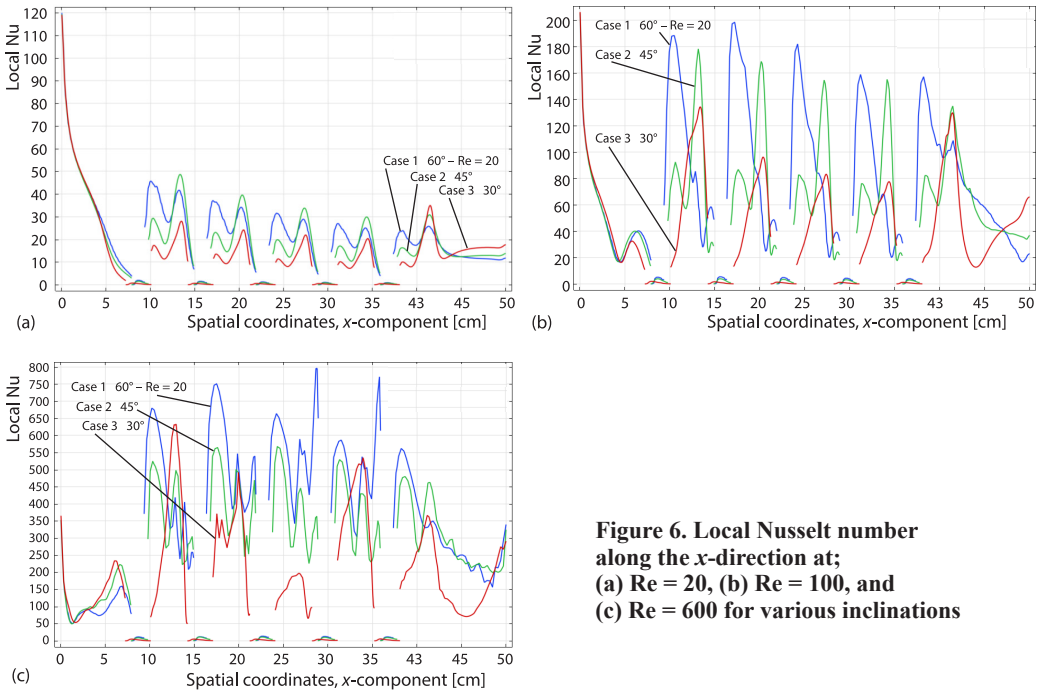

Figure 6. Local Nusselt number along the *x*-direction at; (a) Re = 20, (b) Re = 100, and (c) Re = 600 for various inclinations

relatively low peaks. Despite the weak convective activity, the *L*-shaped obstacles still induce minor flow disturbances that locally enhance heat transfer. Among the tested configurations, the 60° inclination exhibits the highest peaks, indicating that even under low flow conditions, steeper angles create more pronounced boundary-layer disruption. The 45° inclination yields intermediate results, while the 30° inclination shows the lowest and most uniform profile, due to its reduced ability to disturb the flow. Between the peaks, the Nusselt number drops to very low values, signaling zones of flow reattachment and boundary-layer growth.

As the Reynolds number increases to 100, convective mechanisms become more influential. Figure 6(b) shows that the local Nusselt number profile develops more distinct and sharper peaks, corresponding to stronger vortex formation and boundary-layer thinning near each obstacle. The 60° inclination continues to produce the highest Nusselt values, benefiting from increased flow disturbance and mixing. The 45° inclination also shows strong performance, with slightly lower but still significant peaks. The 30° case, while improved compared to Re = 20, remains the least effective. At this intermediate Re number, the ability of the obstacles to generate organized re-circulation zones and enhance local heat transfer becomes increasingly important.

At Re = 600, the flow approaches a highly transitional or turbulent state. As depicted in fig. 6(c), the local Nusselt number profile becomes highly oscillatory, with sharp, irregular peaks and fewer deep valleys. The 60° inclination demonstrates the most effective heat transfer, with Nusselt number values exceeding 800. This is attributed to strong flow separation and intense vortex generation, which sustain boundary-layer disruption and promote cold fluid penetration along the wall. The 45° case performs comparably well, and in some locations even surpasses 60°, likely due to optimal interaction between the main flow and the obstacles. Although the 30° inclination still results in lower peaks, its performance improves significantly at this Reynolds number, highlighting that even shallow angles can benefit from turbulence-in-

duced mixing. Notably, the valleys remain elevated, indicating that the thermal boundary-layer does not fully recover between obstacles.

Overall, the periodic local Nusselt number variations confirm the strong influence of the inverted *L*-shaped obstacles on thermal performance. The inclination angle and Reynolds number jointly dictate the extent of boundary-layer disturbance and vortex strength. While lower inclinations are less effective, particularly at low Reynolds numbers, the 60° inclination consistently provides superior heat transfer enhancement across all flow regimes, making it the optimal configuration for maximizing convective performance in the studied geometry.

The average Nusselt number, Nu_{av}, serves as a comprehensive indicator of heat transfer performance, integrating the effects of obstacle geometry and flow intensity across the entire channel. As presented in fig. 7, the variation of Nu_{av} with Reynolds number and inclination angle (30°, 45°, and 60°) reveals significant insights into thermal enhancement mechanisms. At all Reynolds numbers, the Nu_{av} increases with both flow rate and obstacle inclination. For instance, at Re = 20, increasing the inclination from 30° to 45° improves heat transfer by 33% (from 13.94-18.51), and further increasing it to 60° results in a 53% gain over the 30° case. Similarly, at Re = 100, the 45° case enhances performance by 42.7% compared to 30°, while the 60° configuration achieves a 78.9% improvement.

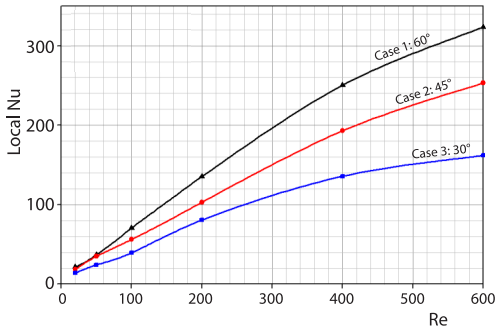

Figure 7. Influence of obstacle inclination and flow rate on average Nusselt number

At higher Reynolds numbers, the impact of inclination becomes even more pronounced. At Re = 400, the 60° set-up achieves an average Nusselt number of 250.42, which is 84.5% higher than the 135.66 observed for 30°, and 29.7% greater than the 193.01 obtained for 45°. At Re = 600, this trend persists: the 60° inclination outperforms the 30° and 45° cases by 99.5% and 27.7%, respectively. These significant differences underline the effectiveness of steeply inclined *L*-shaped obstacles in disrupting the flow, enhancing mixing, and thinning the thermal boundary-layer, especially under strong convective regimes.

Even at lower Reynolds numbers, where conduction dominates and convection is weaker, the relative gains from obstacle inclination remain noticeable. At Re = 50, the increase from 30° to 60° yields a 51.3% enhancement, confirming that even modest increases in geometric aggressiveness can yield measurable thermal benefits under laminar conditions.

Overall, the data confirm a synergistic relationship between obstacle inclination and Reynolds number. The 60° inclination consistently provides the highest Nu_{av} across the entire Reynokds number range, with performance improvements exceeding 90% in some cases compared to the shallowest configuration. This makes it the optimal design in the tested range for maximizing convective heat transfer in channels with periodic *L*-shaped obstacles.

Conclusions

A detailed numerical study was carried out to evaluate the effect of inverted *L*-shaped obstacle inclination and flow rate on heat transfer enhancement in a rectangular D-channel. The conclusiones are as follows.

- The use of periodically arranged inclined obstacles introduces localized flow disturbances, generating re-circulation zones and impingement regions that significantly enhance convective heat transfer.

- Increasing the Reynolds number leads to thinner thermal boundary-layers, stronger vortex activity, and elevated local and average Nusselt numbers across all cases.
- Among the three tested inclination angles (30°, 45°, and 60°), the 60° configuration consistently delivered superior performance, especially at higher Reynolds numbers. At Re = 600, it outperformed the 30° configuration by approximately 99.5% in terms of average Nusselt number.
- Temperature contours and local Nusselt profiles confirmed the role of inclination angle in controlling flow reattachment, mixing intensity, and downstream cooling effectiveness.
- The study demonstrates that geometric tuning of obstacle inclination offers a simple and efficient passive method for boosting thermal performance in internal flow applications, particularly under moderate to high flow conditions.

Future research may extend this work by examining pressure drop penalties, optimizing obstacle shape and spacing, or employing non-Newtonian or nanofluid working fluids to further improve thermal-hydraulic performance.

Acknowledgment

Princess Nourah bint Abdulrahman University Researchers Supporting Project number (PNURSP2025R826), Princess Nourah bint Abdulrahman University, Riyadh, Saudi Arabia.

References

[1] Menni, M., *et al.*, Enhancing Heat Transfer Performance: A Comprehensive Review of Perforated Obstacles, *Revista Mexicana de Fisica*, *71* (2025), 3, 030601-1
[2] Moradi, I., D'Orazio, A., Lattice Boltzmann Method Pore-scale simulation of fluid-flow and heat transfer in porous media: Effect of Size And Arrangement of Obstacles into a Channel, Engineering Analysis with Boundary Elements, *152* (2023), July, pp. 83-103
[3] Mohankumar, V., Prakash, K. A., Effect of Axis Ratio and Geometric Location of The Elliptical Obstacles on Thermo-Fluid Dynamic Characteristics in A Double Forward-Facing Step Channel, *International Journal of Numerical Methods for Heat & Fluid-Flow*, *35* (2025), 7, pp. 2543-2576
[4] Nitin, S., Chhabra, R. P., Non-Isothermal Flow of a Power Law Fluid Past a Rectangular Obstacle (of Aspect Ratio 1×2) in a Channel: Drag and Heat Transfer, *International Journal of Engineering Science*, *43* (2005) 8-9, pp. 707-720
[5] Hameed, A. F., *et al.*, Thermal and Hydraulic Performance of Serpentine Mini-Channel Heat Sink: Influence of Integrated Obstacles in Curved Channels, *International Journal of Thermal Sciences*, *215* (2025), 110006
[6] Akbari, O. A., *et al*., Investigating the Heat Transfer and Two-Phase Fluid-Flow of Nanofluid in the Rough Micro-Channel Affected by Obstacle Structure Changes, *International Journal of Thermofluids*, *24* (2024), 100974
[7] Alshukri, M. J., *et al*., Convective Heat Transfer Analysis in Turbulent Nanofluid-Flow through a Rectangular Channel with Staggered Obstacles: A Numerical Simulation, *International Journal of Thermofluids*, *23* (2024), 100753
[8] Ghoulam, O., *et al*., Heat Transfer Improvement in Turbulent Flow Using Detached Obstacles in Heat Exchanger Duct, *International Journal of Thermofluids*, *27* (2025), 101225
[9] Akhter, R., *et al.*, Data Analysis of Thermal Performance and Irreversibility of Convective Flow in Porous-Wavy Channel Having Triangular Obstacle under Magnetic Field Effect, *Heliyon*, *10* (2024), 14, e34580
[10] Yaseen, D. T., *et al*., Controlling Convective Heat Transfer of Shear Thinning Fluid in a Triangular Enclosure with Different Obstacle Positions, *Case Studies in Thermal Engineering*, *61* (2024), 105003
[11] Ren, X. H., *et al*., Thermal Buoyancy Driven Flows Inside the Solar Chimney: Volume Flow and Heat Transfer Rates Effected through Immersed Solid Obstacles with Different Thermal Conductivity and Flushly-Inserted Discrete Heating Elements, *Energy*, *322* (2025), 135527
[12] Khan, Z. H., *et al*., Mixed Convection Flow in a Channel with a Dimpled Section and Adiabatic Cylindrical Obstacle under the Influence of Magnetic and Joule Effects, *Results in Physics*, *49* (2023), 106550

[13] Mirahsani, S., *et al*., Optimal Design of an Array of Porous Obstacles in a Partially Heated Channel Using Lattice Boltzmann Method for The Heat Transfer Enhancement, *International Communications in Heat and Mass Transfer*, *143* (2023), 106737
[14] Pakhomov, M. A., The RANS Simulation of Heat Transfer in a Mist Turbulent Flow over an Obstacle, *International Journal of Thermal Sciences*, *199* (2024), 108913
[15] Han, J., *et al*., Influence of Obstruction's Unilateral Length on Flow and Heat Transfer Performance of Micro-Channel Heat Sinks with Flow Obstructions, *Case Studies in Thermal Engineering*, *50* (2023), 103509
[16] Barman, A., Dash, S. K., Effect of Obstacle Positions for Turbulent Forced Convection Heat Transfer and Fluid-Flow over a Double Forward Facing Step, *International Journal of Thermal Sciences*, *134* (2018), Dec., pp. 116-128
[17] Tassone, A., *et al*., Magnetohydraulic Flow in a Rectangular Channel Filled with Stream-Wise Obstacles, *Fusion Engineering and Design*, *197* (2023), 114066
[18] Hammid, S., *et al*., Overall Assessment of Heat Transfer for a Rarefied Flow in a Micro-Channel with Obstacles Using Lattice Boltzmann method, *Comput. Model. Eng. Sci*, *138* (2024), 1, pp. 273-299
[19] Pirouz, M. M., *et al*., Lattice Boltzmann Simulation of Conjugate Heat Transfer in a Rectangular Channel with Wall-Mounted Obstacle, *Scientia Iranica*, *18* (2011) 2, pp. 213-221
[20] Selimefendigil, F., Oztop, H. F., Forced Convection in a Branching Channel with Partly Elastic Walls and Inner L-Shaped Conductive Obstacle under the Influence of Magnetic Field, *International Journal of Heat and Mass Transfer*, *144* (2019) 118598
[21] Salmi, M., *et al*., The CFD-Based Simulation and Analysis of Hydrothermal Aspects in Solar Channel Heat Exchangers with Various Designed Vortex Generators, *Computer Modelling in Engineering & Sciences*, *126* (2021), 1, pp. 147-173
[22] Maouedj, R., *et al*., Simulating the Turbulent Hydrothermal Behavior of Oil/MWCNT Nanofluid in a Solar Channel Heat Exchanger Equipped with Vortex Generators, *Computer Modelling in Engineering & Sciences*, *126* (2021), 3, pp. 855-889
[23] Menni, Y., *et al*., Combination of Baffling Technique and High-Thermal Conductivity Fluids to Enhance the Overall Performances of Solar Channels, *Engineering with Computers*, *38* (2022), Suppl. 1, S607-S628
[24] Chamkha, A. J., *et al*., Thermal-Aerodynamic Performance Measurement of Air Heat Transfer Fluid Mechanics over S-Shaped Fins in Shell-and-Tube Heat Exchangers, *Journal of Applied and Computational Mechanics*, *7* (2021), 4, pp. 1931-1943
[25] Medjahed, D. M., *et al*., Details on the Hydrothermal Characteristics Within a Solar-Channel Heat-Exchanger Provided with Staggered T-Shaped Baffles, *Energies*, *14* (2021), 20, 6698
[26] Comolet, R., *Mécanique Expérimentale des Fluides*, 4th ed., Dunod, Paris, France, 2006

Paper submitted: March 22, 2025
Paper revised: June 29, 2025
Paper accepted: July 29, 2025

2025 Published by the Vinča Institute of Nuclear Sciences, Belgrade, Serbia.
This is an open access article distributed under the CC BY-NC-ND 4.0 terms and conditions.